

# ULTRASONIC TOMOGRAPHY FOR IMAGING REINFORCEMENT STEEL IN CONCRETE BRIDGE GIRDERS

Stephen J. Norton, Dean Keiswetter and I. J. Won

Geophex, Ltd., Raleigh, NC 27603; norton@geophex.com

## ABSTRACT

A new technique is proposed for assessing the quantity and distribution of reinforcing steel in concrete bridge girders. Because of the high impedance contrast between concrete and steel, images derived from conventional (ray-based) tomographic algorithms can suffer severe degradation due to multiple scattering between the rebar components and the girder boundary. This degradation can significantly affect image clarity and resolution. A full-wave, iterative algorithm was investigated that is not affected by the image degradation associated with ray-based algorithms resulting from the neglect of multiple scattering and multi-path, refraction around low-speed regions, shadow zones, etc. In the full wave approach, boundary interactions are also accounted for. Finally, a priori information on the properties of concrete and steel can be incorporated.

## I. INTRODUCTION

The Army would like to develop a non-destructive technology for evaluating the Military Load Capacity (MLC) of bridges. An accurate assessment of the MLC of an unfamiliar bridge is necessary to determine whether the bridge can sustain troop and vehicle movement. The most critical indicator of a bridge's MLC is the quantity of internal steel reinforcement in the concrete girders supporting the bridge. The Army has proposed developing imaging techniques for visualizing the internal steel girder reinforcement.

A promising methodology identified by the Army for this purpose is ultrasonic tomography. This technique employs sources and receivers of ultrasound spaced around the boundaries of the girder. In conventional ultrasonic tomography, pulses of ultrasound are launched into the material and travel time measurements are recorded between pairs of transmitting and receiving transducers. Such measurements, recorded over multiple intersecting paths, give rise to a system of linear equations that can be solved for the distribution of velocity within the material. One drawback of this approach is that it assumes a ray-based model of ultrasonic propagation, which neglects refraction and scattering of the ultrasonic signals. Essentially, conventional ray-based tomography is the ultrasonic analogue of x-ray tomography.

Geophex has conducted a theoretical investigation into the benefits of developing a more rigorous, wave-equation based ultrasonic imaging algorithm for imaging reinforcing steel in concrete girders. Because of the high impedance contrast between concrete and steel, images derived from conventional (ray-based) tomographic algorithms will suffer severe degradation due to multiple scattering between the rebar components as well as the girder boundary. This degradation will significantly affect image clarity and resolution. We have performed simulations of an algorithm based on the wave equation. This approach is computationally slower than ray-based schemes, but has several potential advantages. The method is not affected by the image degradation associated with ray-based algorithms resulting from the neglect of multiple scattering and multi-path, refraction around low-speed regions, shadow zones, etc. In the full wave approach, boundary interactions are also accounted for. Finally, a priori information on the properties of concrete and steel can be incorporated. Both time-domain and frequency-domain versions of these imaging algorithms can be employed, each with its unique advantages and limitations.

Conventional travel-time tomography has been examined as a method of visualizing the condition of concrete and detecting the presence of voids and rebar (Atkinson and Schuller,

1994). These authors point out that a ray-based model, in which refraction is neglected, seems adequate for imaging concrete with small material contrasts, but correction for refraction is required for higher contrasts (e.g., steel in concrete). Even then, a ray-based model suffers serious limitations that degrade image accuracy and resolution. This is because the ray equation is a reasonable approximation only when the scale of the spatial variations is long compared to a wavelength, and this condition is violated in high-contrast, composite materials such as concrete/rebar. As noted, ray-based schemes break down for several reasons: (1) the neglect of diffraction, (2) failure to account for multi-path and multiple scattering, (3) the tendency of rays to avoid low speed zones, (4) failure to penetrate voids, and (5) the creation of shadow zones.

In principle, all of these problems can be overcome by employing a diffraction or full-wave imaging approach based on the wave equation. Not only is the wave equation a more rigorous propagation model than ray tracing, but it accounts for material variations in both density and velocity, as well as for diffraction and multiple-scattering effects.

## **II. LINEAR DIFFRACTION TOMOGRAPHY**

A wave equation based algorithm that is expected to perform better than ray-based tomography is diffraction tomography. Such an algorithm is derived as follows.

1. A wave equation is written down that explicitly contains the medium's parameters. The spatial variation (or image) of these parameters is unknown and to be determined.
2. The wave equation is transformed into an integral equation containing a Green's function. This integral equation is exact, but nonlinear in the material parameters.
3. The integral equation is linearized using the Born approximation.
4. The linearized integral equation is converted to a matrix equation by discretization and then solved using a standard linear-system solver. In certain simple geometries, the integral equation can be explicitly inverted using Fourier methods (Norton and Linzer, 1981). The latter (analytical) approach will not be applicable to the girder problem because of the girder's finite boundaries.

A limitation of diffraction tomography is that it performs best under weak scattering conditions, that is, it assumes relatively small contrasts in material properties. Under strong scattering conditions, the images can suffer considerable distortion.

## **III. FULL-WAVE ALGORITHM BASED ON ITERATION**

A full-wave approach does not assume weak scattering (or small material contrasts). In this approach, steps (1) and (2) above are performed, but not the linearization in step (3). The resulting integral equation is exact, but nonlinear in the unknown material parameters. An image of the material parameters is obtained by iterating the forward scattering problem. This involves the following steps.

1. An initial estimate of the material parameters inside the object is obtained. This initial guess could correspond, for example, to a uniform concrete girder with no rebar or a crude image based on a fast linear inversion (e.g., diffraction tomography).
2. Given a set of ultrasonic sources and receivers, the received signals are predicted on the basis of the above parameter estimate using a numerical wave-propagation algorithm (the "forward algorithm"). A variety of forward algorithms are possible, e.g., based on solving an integral equation or on solving a finite-difference approximation to the wave equation. The latter approach is generally faster for time-dependent or broadband scattering problems.
3. By iteration, the algorithm then attempts to minimize a global misfit, typically the mean-square error, between the actual and predicted data subject to a priori constraints. For each iteration, the forward algorithm is re-computed and the material parameters are adjusted to drive the mean-

square error to a minimum. The final result is an image that best predicts the measurements. This process in principle gives rise to a quantitative image of the material parameters, in contrast to, for example, phased array imaging, which produces a qualitative image of material contrasts.

4. At each iteration, one needs to compute the gradient of the mean-square error with respect to the material parameters in order to “slide down hill” on the error surface in parameter space. That is, if we divide the girder cross-section into a set of pixels, we require the partial derivatives of the mean-square error with respect to each pixel value.

Until recently, this gradient evaluation has been by far the most time consuming part of the calculation. The partial derivatives can be computed in a brute-force manner using finite differences, but this is computationally very expensive. For example, if there are  $N$  pixels in the image, the gradient calculation would require on the order of  $N$  forward scattering calculations per iteration. However, a far more efficient method for computing these derivatives, known as the “adjoint method,” requires only two forward solutions per iteration and is independent of  $N$ . As a result, the adjoint method has recently become common in the solution of large-scale nonlinear inverse problems in geophysics and other fields. One author of this paper has applied this method to a variety of nonlinear inverse problems (Norton, 1988; Norton and Bowler, 1993; Norton, 1997). A recent article describes a general theory of iterative nonlinear inversion algorithms that exploits this approach (Norton, 1999).

Once the gradient of the mean-square error is computed, any descent algorithm can be used to minimize the global error, such as a quasi-Newton or conjugate-gradient method. In the simulation described below, a conjugate-gradient algorithm was employed.

#### **IV. INCORPORATION OF A PRIORI INFORMATION**

An advantage of iterative schemes in general is their ability to impose a priori constraints at each iteration. There are several ways that this can be accomplished in the girder imaging problem. One approach is to constrain the material's velocity (and/or density) to two values only: that of concrete and that of steel. The actual values of these two velocities can also be regarded as unknowns. A second approach is to employ a Bayesian formulation of the image reconstruction problem. In this case, one assumes that the a priori probability of the unknown material parameters is bimodal or double peaked, in which one peak corresponds to that of concrete and the other to steel. That is, a histogram of pixel values should cluster around two peaks corresponding to the properties of concrete and steel.

#### **V. FREQUENCY-DOMAIN VERSUS TIME-DOMAIN ALGORITHMS**

Either a frequency-domain or time-domain algorithm can be employed for imaging, each with its own advantages. In a frequency-domain approach, single-frequency illumination is used and amplitude and phase measurements are recorded for a number of source/receiver combinations. Using coherent detection techniques, an accurate phase measurement is easier to achieve than, for example, an accurate transit-time measurement that requires high signal bandwidth. In practice, a narrow band burst would be used of sufficient length to define the signal phase accurately. A time-domain algorithm, on the other hand, employs the full transient waveform, not just the time of first arrival. As a result, fewer source/receiver combinations would be expected compared to single-frequency or ray-based methods, since spatial information is conveyed by the full waveform.

#### **VI. EXAMPLE USING SIMULATED DATA**

As an illustration, consider a two-dimensional imaging problem in which the velocity only is assumed to vary over a cross-sectional region of a concrete girder. We assume for simplicity that the density is constant and that attenuation can be ignored. Both attenuation and density variations can be incorporated without difficulty. We consider here a frequency-domain imaging

problem in which a single frequency is used for illumination. We emphasize that a similar approach can be applied in the time-domain to treat transient signals of arbitrary shape, duration and bandwidth.

In this simulation, the following scenario was assumed. We considered a 2-D square imaging domain (Fig. 1), 16 cm by 16 cm, divided into 16 by 16 one  $\text{cm}^2$  pixels, giving a total of  $N = 256$  unknowns. This is rather coarse resolution, but the number of pixels can be easily increased at the expense of longer run times. The hypothetical object consisted of a square cross-sectional region of homogeneous concrete of speed 4000 m/sec, with a square void (indicated by black in the figure), and two embedded pieces of rebar of square cross section of speed 6000 m/s (indicated by white in the figure). Nine sources (marked by X's) and 48 receivers (marked by O's) were spaced on three sides of the girder as shown in Fig. 1. The wavelength was assumed to be 1 cm in the concrete, corresponding to a frequency of 400 kHz.

Data were simulated by transmitting sequentially from each source transducer and recording with all receiving transducers, giving a total of 432 complex (amplitude and phase) measurements. The conjugate-gradient algorithm was then applied to the simulated data and the resulting image is shown in Fig. 2 after 20 iterations of the algorithm. Each iteration took about 5 minutes on a 200 MHz PC.

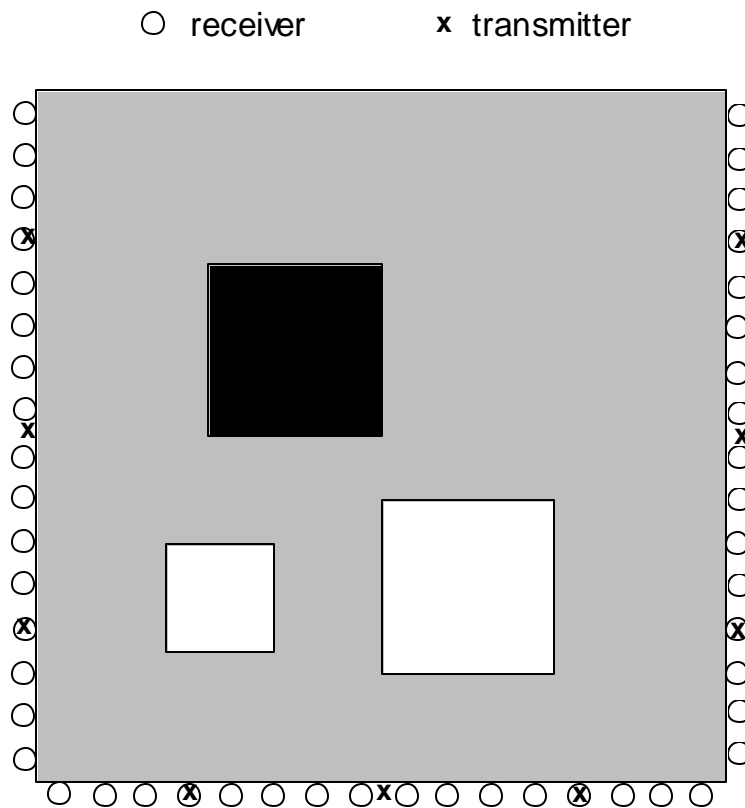


Fig. 1. Cross-sectional region of a hypothetical concrete girder of velocity 4000 m/s with a square void (black) with two square rebar (white) of 6000 m/s. X's mark sources and O's mark receivers.

Although this problem is idealized, it gives a reasonable indication of the kind of resolution and accuracy that can be expected. The algorithm converges rapidly to the correct quantitative values of velocity and can be shown to be robust against noise in the data. Finally, the full-wave

algorithm gives a very good image even when access is restricted to three sides. For a ray-based approach, three-sided access is more problematic since only transmitted paths are considered.

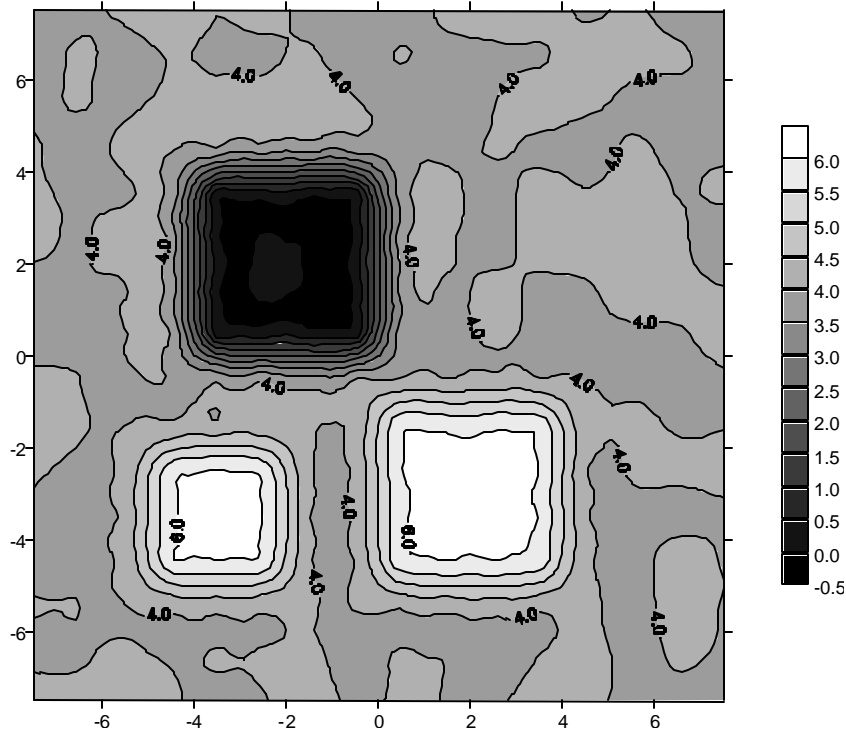


Fig. 2. Full-wave reconstruction of the object shown in Figure 1 after 20 iterations. Units are thousands of meters/sec.

## VII. EXTENSIONS OF THE THEORY

The latter example was meant as a simple illustration of the full-wave algorithm. It is relatively easy to extend the theory merely by modifying the wave equation. We list below several possible extensions.

1. Time-domain inversion. Here the starting point for the algorithm is the time-dependent wave equation. The theory for computing the gradient of the mean-square error remains essentially unchanged. Details of the time-domain version of the inverse problem can be found in (Norton, 1999).
2. Density and velocity imaging. In this case, the density in the wave equation is allowed to be spatially dependent as well as the velocity. Density and velocity are both imaged.
3. Attenuation. Wave attenuation can be readily accounted for by including a damping term (i.e., a first derivative term) in the wave equation.
4. Extension to 3-D Imaging. In theory, the generalization to three dimensions is straightforward, in which 2-D arrays would replace linear arrays and a volume instead of a cross sectional region would be imaged. Data acquisition times and computer processing times would increase by perhaps another order of magnitude.
5. Extension to Shear-Wave Imaging. Horizontally-polarized shear waves (SH waves) could be employed to image the shear velocity (and density). If the rebar runs parallel to the boundaries,

then shear waves polarized parallel to the boundaries will not, in principle, mode convert upon reflection. The resulting wave equation (expressed in terms of a scalar shear potential) is particularly simple and contains only the shear velocity and density. The price paid, however, is the need to use transducers designed to transmit and receive shear waves.

### VIII. SUMMARY

The wave equation based algorithm described here is capable of providing quantitatively more accurate images than conventional imaging schemes based on linear approximations (e.g., travel-time tomography). Although the disadvantage of this approach is its greater computational demands, this limitation is becoming less of an obstacle as computing costs continue to decline.

### REFERENCES

- Atkinson, R. H., and Schuller, M. P., 1994, Characterization of Concrete Condition using Acoustic Tomographic Imaging: Phase I SBIR Report (US Nuclear Regulatory Commission, Contract No. NRC-04-93-094).
- Norton, S. J., and Linzer, M., 1981, Ultrasonic Reflectivity Imaging in Three Dimensions: Exact Inverse Scattering Solutions for Plane, Cylindrical, and Spherical Apertures: IEEE Trans. Biomed. Eng., **BME-28**, 202-220.
- Norton, S. J., 1988, Iterative Seismic Inversion: Geophys. J. Int., **94**, 457-468.
- Norton, S. J., and Bowler, J. R., 1993, Theory of eddy current inversion: J. Appl. Phys., **73**, 501-512.
- Norton, S. J., 1997, A general nonlinear inverse transport algorithm using forward and adjoint flux computations: IEEE Trans. Nucl. Sci. Eng., **NS-44**, 153-162.
- Norton, S. J., 1999, Iterative inverse scattering algorithms: Methods of computing Frechet derivatives: J. Acoust. Soc. Amer., **106**, 2653-2660.